SICE Annual Conference 2014
September 9-12, 2014, Hokkaido University, Sapporo, Japan

# Fuel Consumption Optimization for a Power-Split HEV via Gain-Scheduled Model Predictive Control

Hitoshi Iyama[1†] and Toru Namerikawa[1]

[1]Department of System Design Engineering, Keio University, Kanagawa, Japan
(Tel: +81-45-563-1151; E-mail: hitoshii@nl.sd.keio.ac.jp , namerikawa@sd.keio.ac.jp)

**Abstract:** In this paper, we propose a fuel consumption optimization technique for a power-split hybrid electric vehicle (HEV) via gain-scheduled model predictive control. The control algorithms for the hybrid powertrain choose the power split between the internal combustion engine and electric motor of the HEV in order to minimize the fuel consumption. The operating conditions of the HEV change during driving in real time by road conditions and driver demand. Therefore, it is necessary to have optimal control in real time and to consider the time-varying motor condition. We model an HEV and propose a gain-scheduled model predictive control for a power-split HEV. Using the proposed technique, the optimal fuel consumption for a power-split HEV is achieved. Finally, the proposed approach is validated by numerical simulations.

**Keywords:** Gain-Scheduled Model Predictive Control, Hybrid Electric Vehicle, Optimal Control.

## 1. INTRODUCTION

In recent years, the number of cars has been increasing in the world. An environmental technology for cars has been developed in response to environmental concerns and problems of rising fuel cost. The hybrid electric vehicle (HEV) is provided by electric motors and an internal combustion engine and is reduced emissions and fuel consumption by combining their output[1]. The improvement of fuel economy is achieved by using surplus energy that is recovered from engine power and the regenerative energy reused, as shown in Fig. 1, and allow running a smaller combustion engine in a higher efficiency region. However, the control of the HEV with a battery and two driving forces is more complex than a conventional car.

Therefore, the control of the HEV to optimize fuel consumption is being actively studied [2][3][4][5][6]. Therein, the model predictive control [2] is believed to be an effective means. However, in previous studies, the state of the battery, which depends on the varying motor speed, cannot be simulated. The controlling the battery within its physical constraints is necessary to express the varying state of motor speed.

In this paper, we propose a fuel consumption optimization technique for a power-split HEV as shown in Fig. 2 via gain-scheduled model predictive control [7]. We make possible an optimal control for a variable state system and represent the varying state by combining gain-scheduled model with conventional model predictive control. Thus, it is possible to optimize fuel consumption for an HEV considering not only the state of the engine, EM1, and EM2 but also the state of the battery. The scheduled parameter used in the gain-scheduled control is obtained by linear interpolation between the minimum and maximum of the EM1 and EM2 rotational speed.

At first, we model a power-split HEV and describe about the general model predictive control. Then the gain-scheduled model predictive control proposes. Finally, the proposed control law is validated by a numerical simulation.

† Hitoshi Iyama is the presenter of this paper.

## 2. PROBLEM SETTING

### 2.1. Fuel Economy Optimization Problem

In this paper, the fuel economy optimization problem is considered for the optimal distribution of power in the HEV powertrain to maximize fuel economy and combustion efficiency. This problem needs to consider not only the optimization of fuel consumption but also the constraint of the battery state, drivability.

### 2.2. HEV Modeling

In this section, we consider the model of a power-split HEV as shown in Fig. 2.

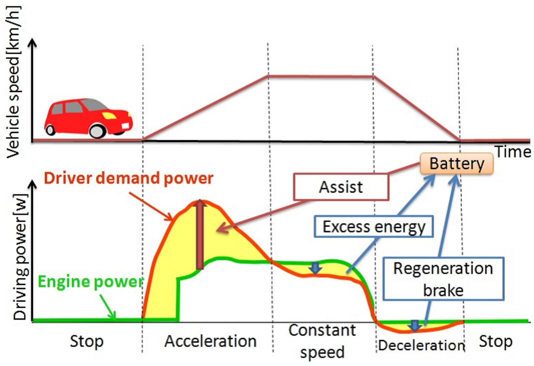


Fig. 1 Improvement of fuel economy

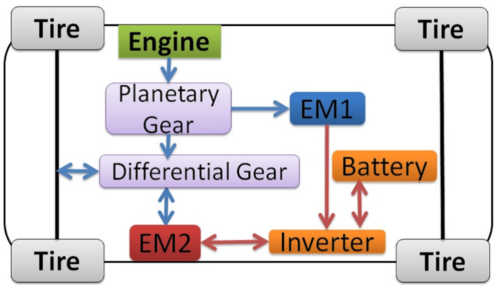


Fig. 2 Power-split HEV

### 2.2.1. Vehicle Dynamics

The motion of the HEV is formulated as

$$M\dot{v}(t) = f_d(t) - f_a(t) - f_r(t) - f_g(t) \tag{1}$$

where

$$f_d(t) = \frac{\tau_d(t)}{R_w} \quad (driving\ force), \tag{2}$$

$$f_a(t) = \frac{1}{2}\rho A_f C_d v^2(t) \quad (air\ resistance), \tag{3}$$

$$f_r(t) = \mu M g \cos(\theta(t)) \quad (rolling\ resistance), \tag{4}$$

$$f_g(t) = M g \sin(\theta(t)) \quad (gradient\ resistance), \tag{5}$$

here $M$[kg] is the vehicle weight and $R_w$[m] is the tire radius, $\rho[\mathrm{kg/m^3}]$ is the air density, $C_d$ is the air resistance coefficient, $A_f[\mathrm{m^2}]$ is the vehicle frontal projected area, $\mu$ is the rolling resistance coefficient, $g[\mathrm{m/s^2}]$ is the gravitational acceleration, $\theta$[rad] is the road gradient, $v$[m/s] is the vehicle speed, $\tau_d$[Nm] is the driver-demanded torque, $t[s]$ is time. The driver-demanded torque, which is a measurable disturbance to the car, becomes Eq. (6) based on Eq. (1).

$$\tau_d(t) = R_w(M\dot{v}(t) + \frac{1}{2}\rho A_f C_d v^2(t) + Mg\cos(\theta(t)) + Mg\sin(\theta(t))) \tag{6}$$

### 2.2.2. Powertrain Dynamics

We formulate the equation of state of EM1, EM2, and the engine to configure the powertrain of the HEV. EM1, EM2, and the engine are connected as shown in Fig. 2 by planetary gears. The relationships among the speed of the powertrain components are formulated as [8][9]

$$R_r\omega_{em2}(t) + R_s\omega_{em1}(t) = (R_r + R_s)\omega_{eng}(t) \tag{7}$$

where $\omega_{em1}$[rad/s], $\omega_{em2}$[rad/s], and $\omega_{eng}$[rad/s] are EM1, EM2, and the engine rotational speed, respectively. $R_s$[m], $R_r$[m] are sun gear and ring gear radius, respectively. Then, the motion equation of rotation for EM1, EM2, and the engine are shown as

$$I_{em1}\dot{\omega}_{em1}(t) = \tau_{em1}(t) + f_p(t)R_s, \tag{8}$$

$$I_{em2}\dot{\omega}_{em2}(t) = \tau_{em2}(t) - \frac{\tau_d(t)}{G_f} + f_p(t)R_r, \tag{9}$$

$$I_{eng}\dot{\omega}_{eng}(t) = \tau_{eng}(t) - f_p(t)(R_s + R_r), \tag{10}$$

where $I_{em1}[\mathrm{kg \cdot m^2}]$, $I_{em2}[\mathrm{kg \cdot m^2}]$, and $I_{eng}[\mathrm{kg \cdot m^2}]$ are inertia moments of EM1, EM2, and the engine, $G_f$ is the differential gear ratio, $f_p$[N] is the interaction force caused by contact with the planetary gear, $\tau_{em1}$[Nm], $\tau_{em2}$[Nm], and $\tau_{eng}$[Nm] are EM1, EM2, and engine torque, respectively. $f_p(t)$[N] is expressed in Eq. (11) as follows from Eqs. (7) and (8).

$$f_p(t) = \frac{I_{em1}}{R_s^2}[(R_r+R_s)\dot{\omega}_{eng}(t) - R_r\dot{\omega}_{em2}(t)] - \frac{\tau_{em1}(t)}{R_s} \tag{11}$$

The motion equations for EN2 and engine are formulated in Eq. (12) as follows from Eqs. (9), (10), and (11).

$$\begin{bmatrix} I_{eng} + \left(\frac{R_r+R_s}{R_s}\right)^2 I_{em1} & -\frac{R_r(R_r+R_s)}{R_s^2} I_{em1} \\ -\frac{R_r(R_r+R_s)}{R_s^2} I_{em1} & I_{em2} + \left(\frac{R_r}{R_s}\right)^2 I_{em1} \end{bmatrix} \begin{bmatrix} \dot{\omega}_{eng}(t) \\ \dot{\omega}_{em2}(t) \end{bmatrix} = \begin{bmatrix} 1 & \frac{R_r+R_s}{R_s} & 0 \\ 0 & -\frac{R_r}{R_s} & 1 \end{bmatrix} \begin{bmatrix} \tau_{eng}(t) \\ \tau_{em1}(t) \\ \tau_{em2}(t) \end{bmatrix} + \begin{bmatrix} 0 \\ -\frac{1}{G_f} \end{bmatrix} \tau_d(t) \tag{12}$$

### 2.2.3. Battery Dynamics

The battery needs to be controlled within its constraints to prevent over-charging or over-discharging. The state of charge is $soc[\%]$.

$$soc^{min} \leq soc(t) \leq soc^{max} \tag{13}$$

The state equation for the battery can be given as [8][9]

$$\dot{soc}(t) = -\frac{V_{oc} - \sqrt{V_{oc}^2 - 4p_{batt}(t)R_{batt}}}{2C_{batt}R_{batt}} \tag{14}$$

where $C_{batt}$[Ah] is the battery capacity, $p_{batt}$[W] is the battery power , $V_{oc}$[V] is the open circuit voltage, and $R_{batt}[\Omega\ ]$ is the battery resistance. The battery power in Eq. (15) is a function of the rotational speed and torque. Here the efficient of battery charge and discharge are not considered.

$$p_{batt}(t) = \tau_{em1}(t)\omega_{em1}(t) + \tau_{em2}(t)\omega_{em2}(t) \tag{15}$$

Eqs. (14) and (15) represent the relationship between $\dot{soc}$ and $p_{batt}$ in Fig. 3. Therefore, the equation for the battery state can be formulated as Eq. (17), which can be considered from the approximate straight line in Fig. 3.

$$\dot{soc}(t) = S_o p_{batt}(t) \tag{16}$$

$$= S_o(\omega_{em1}(t)\tau_{em1}(t) + \omega_{em2}(t)\tau_{em2}(t)) \tag{17}$$

where $S_o$ is the battery coefficient. This equation for the battery state has time-varying states, which are $\omega_{em1}(t)$ and $\omega_{em2}(t)$.

### 2.2.4. Fuel Consumption Model

We next consider the fuel consumption model. The instantaneous fuel consumption $\dot{m}_f$[g/s] is expressed in Fig. 4 from the relationship between torque and speed. Then, we consider the approximate straight line passing through the origin in Fig. 4. This line can express as

$$\dot{m}_f(t) = E_0\tau_{eng}(t) \tag{18}$$

where $E_0$ is the fuel consumption coefficient, which is average of slop on the each engine rotational speed.

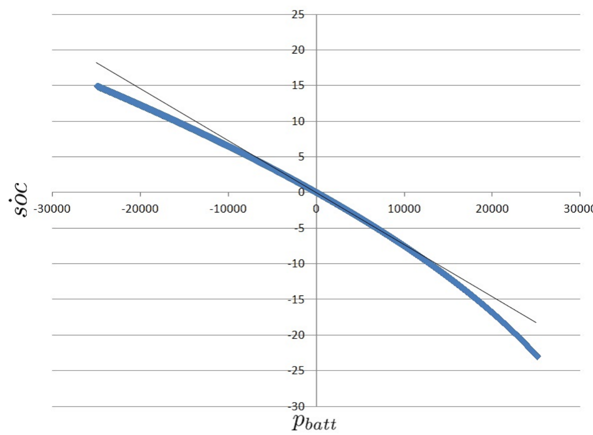


Fig. 3 Soc and battery power

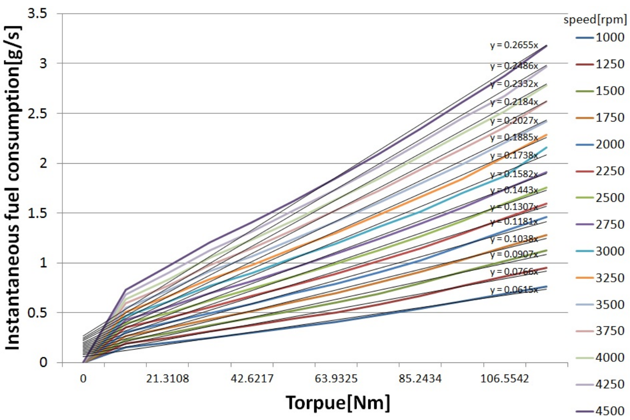


Fig. 4 Fuel consumption

2.2.5. State Space Representation

We show a state-space representation of the HEV by using the equations derived in the previous section. The $\boldsymbol{B}$ matrix is time-varying because the battery has a time-varying state.

$$\begin{aligned}
\dot{\boldsymbol{x}}(t) &= \boldsymbol{A}\boldsymbol{x}(t) + \boldsymbol{B}(t)\boldsymbol{u}(t) + \tilde{\boldsymbol{B}}d(t) && (19)\\
\boldsymbol{y}(t) &= \boldsymbol{C}\boldsymbol{x}(t) + \boldsymbol{D}\boldsymbol{u}(t) && (20)\\
\text{subject to} \quad & \boldsymbol{u}^{min} \leq \boldsymbol{u}(t) \leq \boldsymbol{u}^{max} && (21)\\
& \boldsymbol{y}^{min} \leq \boldsymbol{y}(t) \leq \boldsymbol{y}^{max} && (22)
\end{aligned}$$

where

$$\boldsymbol{x}(t) = \begin{bmatrix} \omega_{eng}(t) \\ \omega_{em2}(t) \\ m_f(t) \\ soc(t) \end{bmatrix}, \boldsymbol{y}(t) = \begin{bmatrix} \omega_{eng}(t) \\ v(t) \\ m_f(t) \\ soc(t) \end{bmatrix}, d(t) = \tau_d(t),$$

$$\boldsymbol{u}(t) = \begin{bmatrix} \tau_{eng}(t) \\ \tau_{em1}(t) \\ \tau_{em2}(t) \end{bmatrix}, \boldsymbol{A} = \boldsymbol{\alpha} \begin{bmatrix} 0 & 0 & 0 & 0 \\ 0 & 0 & 0 & 0 \\ 0 & 0 & 0 & 0 \\ 0 & 0 & 0 & 0 \end{bmatrix},$$

$$\boldsymbol{B}(t) = \boldsymbol{\alpha} \begin{bmatrix} 1 & \frac{R_r + R_s}{R_s} & 0 \\ 0 & -\frac{R_r}{R_s} & 1 \\ E_0 & 0 & 0 \\ 0 & S_o \cdot \omega_{em1}(t) & S_o \cdot \omega_{em2}(t) \end{bmatrix},$$

$$\tilde{\boldsymbol{B}} = \begin{bmatrix} 0 \\ -\frac{1}{G_f} \\ 0 \\ 0 \end{bmatrix}, \boldsymbol{C} = \begin{bmatrix} 1 & 0 & 0 & 0 \\ 0 & \frac{G_f}{R_w} & 0 & 0 \\ 0 & 0 & 1 & 0 \\ 0 & 0 & 0 & 1 \end{bmatrix}, \boldsymbol{D} = \begin{bmatrix} 0 & 0 & 0 \\ 0 & 0 & 0 \\ 0 & 0 & 0 \\ 0 & 0 & 0 \end{bmatrix},$$

$$\boldsymbol{\alpha} = \begin{bmatrix} I_{eng} + \left(\frac{R_r + R_s}{R_s}\right)^2 I_{em1} & -\frac{R_r(R_r + R_s)}{R_s^2} I_{em1} & 0 & 0 \\ -\frac{R_r(R_r + R_s)}{R_s^2} I_{em1} & I_{em2} + \left(\frac{R_r}{R_s}\right)^2 I_{em1} & 0 & 0 \\ 0 & 0 & 1 & 0 \\ 0 & 0 & 0 & 1 \end{bmatrix}^{-1}.$$

## 2.3. Control Purpose

The cost function can be formulated as the quadratic equation that minimizes the deviation of the target value and state.

$$\min_{\boldsymbol{u}(\tau)} J = \int_t^{t+\Delta t} ((\boldsymbol{y}(\tau) - \boldsymbol{r}(\tau))^T \boldsymbol{Q} (\boldsymbol{y}(\tau) - \boldsymbol{r}(\tau)) + \boldsymbol{u}^T(\tau) \boldsymbol{R} \boldsymbol{u}(\tau)) d\tau \quad (23)$$

subject to

$$\begin{aligned}
\dot{\boldsymbol{x}}(t) &= \boldsymbol{A}\boldsymbol{x}(t) + \boldsymbol{B}\boldsymbol{u}(t) + \tilde{\boldsymbol{B}}\boldsymbol{d}(t) && (24)\\
\boldsymbol{y}(t) &= \boldsymbol{C}\boldsymbol{x}(t) + \boldsymbol{D}\boldsymbol{u}(t) && (25)
\end{aligned}$$

$$\begin{aligned}
& \boldsymbol{u}^{min} \leq \boldsymbol{u}(t) \leq \boldsymbol{u}^{max} && (26)\\
& \boldsymbol{y}^{min} \leq \boldsymbol{y}(t) \leq \boldsymbol{y}^{max} && (27)\\
& t \geq 0 \quad , \quad \Delta t > 0 && (28)
\end{aligned}$$

$$\boldsymbol{x}(t) = \begin{bmatrix} \omega_{eng}(t) \\ \omega_{em2}(t) \\ m_f(t) \\ soc(t) \end{bmatrix}, \quad \boldsymbol{y}(t) = \begin{bmatrix} \omega_{eng}(t) \\ v(t) \\ m_f(t) \\ soc(t) \end{bmatrix},$$

$$\boldsymbol{r}(t) = \begin{bmatrix} \omega_{eng_r}(t) \\ \omega_{em2_r}(t) \\ m_{fr}(t) \\ soc_r(t) \end{bmatrix}, \quad \boldsymbol{u}(t) = \begin{bmatrix} \tau_{eng}(t) \\ \tau_{em1}(t) \\ \tau_{em2}(t) \end{bmatrix},$$

$$\boldsymbol{d}(t) = \tau_d(t), \boldsymbol{R} = \begin{bmatrix} R_{\tau_{eng}} & 0 & 0 \\ 0 & R_{\tau_{em1}} & 0 \\ 0 & 0 & R_{\tau_{em2}} \end{bmatrix},$$

$$\boldsymbol{Q} = \begin{bmatrix} Q_{eng} & 0 & 0 & 0 \\ 0 & Q_v & 0 & 0 \\ 0 & 0 & Q_{m_f} & 0 \\ 0 & 0 & 0 & Q_{soc} \end{bmatrix}.$$

where $J$ is the cost function, $\boldsymbol{u}$ is the control input, $\Delta t$ is the elapsed time, $m_{fr}$[g] is the target fuel consumption, $\omega_{eng_r}$[rad/s] is the target engine speed, $\omega_{r_{em2}}$[rad/s] is the target EM2 speed, $soc_r$[%] is the target state of charge, $Q_{eng}, Q_v, Q_{m_f}, Q_{soc}$ are weight of state, and $R_{\tau_{eng}}, R_{\tau_{em1}}, R_{\tau_{em2}}$ are weight of inputs.

# 3. MODEL PREDICTIVE CONTROL

We formulate a general model predictive control [10]. Model predictive control finds the predictive control input that minimizes the deviation of the predicted output and the reference trajectory that exponentially approaches the target value from the current state in the interval. We input only the current value from the optimal calculated control input. In other words, we determine the current input by prediction and optimization in real time. Then, we rewrite this cost function as a quadratic programming problem and calculate the optimization problem.

## 3.1. Cost Function

Model predictive control represents the cost function to be solved in discrete time. The cost function is formulated as

$$\min_{\boldsymbol{u}} J = \sum_{i=0}^{H_p} ||\hat{\boldsymbol{y}}(k+i) - \hat{\boldsymbol{r}}(k+i)||^2_{\boldsymbol{Q}} + \sum_{i=0}^{H_u} ||\Delta \hat{\boldsymbol{u}}(k+i)||^2_{\boldsymbol{R}} \quad (29)$$

subject to

$$\begin{aligned}\hat{\boldsymbol{x}}(k+1+i) &= \boldsymbol{A}\hat{\boldsymbol{x}}(k+i)+\boldsymbol{B}\hat{\boldsymbol{u}}(k+i)\\ &\quad +\tilde{\boldsymbol{B}}\hat{d}(k+i) \qquad (30)\\ \hat{\boldsymbol{y}}(k+i) &= \boldsymbol{C}\hat{\boldsymbol{x}}(k+i)+\boldsymbol{D}\hat{\boldsymbol{u}}(k+i) \qquad (31)\end{aligned}$$

$$\boldsymbol{y}^{min} \le \boldsymbol{y}(k+i) \le \boldsymbol{y}^{max} \qquad (32)$$

$$\boldsymbol{u}^{min} \le \boldsymbol{u}(k+i) \le \boldsymbol{u}^{max} \qquad (33)$$

$$\Delta\hat{\boldsymbol{u}}(k+i) = 0 \quad for \quad i = H_u+1,...,H_p \qquad (34)$$

where $H_u$ is the control horizon, $H_p$ is the predictive horizon, $\hat{\boldsymbol{r}}$ is the reference trajectory, $\hat{\boldsymbol{y}}$ is the predictive output, $k$ is the current time, $i$ is the step, $\boldsymbol{Q}, \boldsymbol{R}$ are weights, $\hat{\boldsymbol{u}}$ is the predictive control input, and $\Delta\hat{\boldsymbol{u}}$ is expressed by $\Delta\hat{\boldsymbol{u}}(k+i) = \hat{\boldsymbol{u}}(k+i) - \hat{\boldsymbol{u}}(k+i-1)$.

### 3.2. Predictive Output

The predictive state and predictive input is given as

$$\begin{aligned}\hat{\boldsymbol{x}}(k+1) &= \boldsymbol{A}\boldsymbol{x}(k)+\boldsymbol{B}\hat{\boldsymbol{u}}(k)+\tilde{\boldsymbol{B}}d(k) \qquad (35)\\ &\vdots\\ \hat{\boldsymbol{x}}(k+H_p) &= \boldsymbol{A}^{H_p}\boldsymbol{x}(k)+\boldsymbol{A}^{H_p-1}\boldsymbol{B}\hat{\boldsymbol{u}}(k)+\cdots\\ &\quad +\boldsymbol{B}\hat{\boldsymbol{u}}(k+H_p-1)+\boldsymbol{A}^{H_p-1}\tilde{\boldsymbol{B}}d(k)\\ &\quad +\cdots+\tilde{\boldsymbol{B}}d(k+H_p-1) \qquad (36)\\ \hat{\boldsymbol{u}}(k) &= \Delta\hat{\boldsymbol{u}}(k)+\boldsymbol{u}(k-1) \qquad (37)\\ &\vdots\\ \hat{\boldsymbol{u}}(k+H_u-1) &= \Delta\hat{\boldsymbol{u}}(k+H_u)+\cdots+\boldsymbol{u}(k-1) \quad (38)\end{aligned}$$

The predicted output is determined by substituting the estimated input and the predicted state from Eq. (39). The predictive output from $\Delta\boldsymbol{U}(k) = [\Delta\hat{\boldsymbol{u}}(k)\cdots\Delta\hat{\boldsymbol{u}}(k+H_u-1)]^T$ is formulated as

$$\boldsymbol{Y}(k) = \boldsymbol{\Psi}\boldsymbol{x}(k)+\boldsymbol{\Upsilon}\boldsymbol{u}(k-1)+\boldsymbol{\Theta}\Delta\boldsymbol{U}(k)+\boldsymbol{\Xi}\boldsymbol{D_m}(k) \qquad (39)$$

subject to

$$\boldsymbol{Y}(k) = \begin{bmatrix}\hat{\boldsymbol{y}}(k+1)\\ \vdots\\ \hat{\boldsymbol{y}}(k+H_p)\end{bmatrix}, \boldsymbol{D_m}(k) = \begin{bmatrix}\hat{d}(k)\\ \hat{d}(k+1)\\ \vdots\\ \hat{d}(H_p-1)\\ \hat{d}(H_p)\end{bmatrix},$$

$$\boldsymbol{\Psi} = \boldsymbol{C}\begin{bmatrix}\boldsymbol{A}\\ \boldsymbol{A}^2\\ \vdots\\ \boldsymbol{A}^{H_u}\\ \boldsymbol{A}^{H_u+1}\\ \boldsymbol{A}^{H_p}\end{bmatrix}, \boldsymbol{\Upsilon} = \boldsymbol{C}\begin{bmatrix}\boldsymbol{B}\\ \boldsymbol{AB}\\ \vdots\\ \sum_{i=0}^{H_u-1}\boldsymbol{A}^i\boldsymbol{B}\\ \sum_{i=0}^{H_u}\boldsymbol{A}^i\boldsymbol{B}\\ \vdots\\ \sum_{i=0}^{H_p-1}\boldsymbol{A}^i\boldsymbol{B}\end{bmatrix},$$

$$\boldsymbol{\Theta} = \boldsymbol{C}\begin{bmatrix}\boldsymbol{B} & 0 & \cdots & 0\\ \boldsymbol{AB}+\boldsymbol{B} & \boldsymbol{B} & \cdots & 0\\ \vdots & \cdots & \ddots & 0\\ \sum_{i=0}^{H_u}\boldsymbol{A}^i\boldsymbol{B} & \cdots & \cdots & \boldsymbol{B}\\ \boldsymbol{B} & 0 & \cdots & 0\\ \sum_{i=0}^{H_p-1}\boldsymbol{A}^i\boldsymbol{B} & \cdots & \cdots & \sum_{i=0}^{H_p-H_u}\boldsymbol{A}^i\boldsymbol{B}\end{bmatrix},$$

$$\boldsymbol{\Xi} = \boldsymbol{C}\begin{bmatrix}\tilde{\boldsymbol{B}} & 0 & \cdots & 0\\ \boldsymbol{A}\tilde{\boldsymbol{B}} & \tilde{\boldsymbol{B}} & \cdots & 0\\ \vdots & \vdots & \ddots & \vdots\\ \boldsymbol{A}^{H_p-1}\tilde{\boldsymbol{B}} & \boldsymbol{A}^{H_p-2}\tilde{\boldsymbol{B}} & \cdots & \tilde{\boldsymbol{B}}\end{bmatrix}.$$

### 3.3. Quadratic Programming Problem

First $\boldsymbol{G}$ and $\boldsymbol{\Phi}$ are given by Eqs. (40) and (41) as

$$\boldsymbol{G} = 2\boldsymbol{\Theta}^T\boldsymbol{Q}\boldsymbol{\varepsilon}(k) \qquad (40)$$

$$\boldsymbol{\Phi} = \boldsymbol{\Theta}^T\boldsymbol{Q}\boldsymbol{\Theta}+\boldsymbol{R} \qquad (41)$$

where $\boldsymbol{\varepsilon}(k)$ is the error in the predicted output and the reference trajectory. The quadratic programming problem is formulated as in Eqs. (42) and (43) with $\boldsymbol{G}$ and $\boldsymbol{\Phi}$.

$$\min_{\Delta\boldsymbol{U}(k)}\left[\frac{1}{2}\Delta\boldsymbol{U}^T(k)\boldsymbol{\Phi}\Delta\boldsymbol{U}(k)-\boldsymbol{G}^T\Delta\boldsymbol{U}(k)\right] \qquad (42)$$

$$\text{subject to} \quad \boldsymbol{\Omega}\Delta\boldsymbol{U}(k) \le \boldsymbol{\omega} \qquad (43)$$

The optimal $\Delta\boldsymbol{U}^*(k)$ is obtained by calculating Eqs. (42) and (43). The prediction control at the current time becomes $\Delta\hat{\boldsymbol{u}}^*(k)$. Then, the optimal solution at the current time is determined by Eq. (44) in accordance with the previous inputs.

$$\boldsymbol{u}(k) = \boldsymbol{u}(k-1)+\Delta\hat{\boldsymbol{u}}^*(k) \qquad (44)$$

The current optimal control value is inputted to the control target.

## 4. GAIN-SCHEDULED MODEL PREDICTIVE CONTROL

The general model predictive control is formulated in the previous section, but it is not possible to handle the time-varying state of the battery. Therefore, we propose a novel controller using gain-scheduled model predictive control [7]. We represent the time-varying state by scheduled parameters and solve the optimization problem.

At first, we decompose $\boldsymbol{B}$ into 4 matrices, as in Eqs. (45)∼(48), including the maximum and minimum values of EM1 and EM2 rotation speed. The $\boldsymbol{B}$ matrix is expressed as $\boldsymbol{B_b^a}$($\boldsymbol{a}$=$\boldsymbol{low}$ or $\boldsymbol{high}$, $\boldsymbol{b}$=$\boldsymbol{em1}$ or $\boldsymbol{em2}$).

$$\boldsymbol{B_{em1}^{low}} = \boldsymbol{\alpha}\begin{bmatrix}1 & \frac{R_r+R_s}{R_s} & 0\\ 0 & -\frac{R_r}{R_s} & 1\\ E_0 & 0 & 0\\ 0 & 2\cdot S_o\cdot\omega_{em1}^{low} & 0\end{bmatrix}, \qquad (45)$$

$$\boldsymbol{B_{em1}^{high}} = \boldsymbol{\alpha}\begin{bmatrix}1 & \frac{R_r+R_s}{R_s} & 0\\ 0 & -\frac{R_r}{R_s} & 1\\ E_0 & 0 & 0\\ 0 & 2\cdot S_o\cdot\omega_{em1}^{high} & 0\end{bmatrix}, \qquad (46)$$

$$\boldsymbol{B_{em2}^{low}} = \boldsymbol{\alpha}\begin{bmatrix}1 & \frac{R_r+R_s}{R_s} & 0\\ 0 & -\frac{R_r}{R_s} & 1\\ E_0 & 0 & 0\\ 0 & 0 & 2\cdot S_o\cdot\omega_{em2}^{low}\end{bmatrix}, \qquad (47)$$

$$\boldsymbol{B^{high}_{em2}} = \boldsymbol{\alpha} \begin{bmatrix} 1 & \frac{R_r+R_s}{R_s} & 0 \\ 0 & -\frac{R_r}{R_s} & 1 \\ E_0 & 0 & 0 \\ 0 & 0 & 2 \cdot S_o \cdot \omega^{high}_{em2} \end{bmatrix}. \quad (48)$$

The four state space representations are utilized for the model predictive control. Then, the optimization problem is calculated by adding up the each quadratic programming problem that multiplied the scheduled parameters. The optimal solution is calculated by Eq. (44).

$$\begin{aligned} \min_{\Delta \boldsymbol{U}(k)} \frac{1}{2} \Bigg[ & \lambda^{low}_{em1} \left[ \frac{1}{2} \Delta \boldsymbol{U}^T(k) \boldsymbol{\Phi^{low}_{em1}} \Delta \boldsymbol{U}(k) - \boldsymbol{G^{low}_{em1}}^T \Delta \boldsymbol{U}(k) \right] \\ & + \lambda^{high}_{em1} \left[ \frac{1}{2} \Delta \boldsymbol{U}^T(k) \boldsymbol{\Phi^{high}_{em1}} \Delta \boldsymbol{U}(k) - \boldsymbol{G^{high}_{em1}}^T \Delta \boldsymbol{U}(k) \right] \\ & + \lambda^{low}_{em2} \left[ \frac{1}{2} \Delta \boldsymbol{U}^T(k) \boldsymbol{\Phi^{low}_{em2}} \Delta \boldsymbol{U}(k) - \boldsymbol{G^{low}_{em2}}^T \Delta \boldsymbol{U}(k) \right] \\ & + \lambda^{high}_{em2} \left[ \frac{1}{2} \Delta \boldsymbol{U}^T(k) \boldsymbol{\Phi^{high}_{em2}} \Delta \boldsymbol{U}(k) - \boldsymbol{G^{high}_{em2}}^T \Delta \boldsymbol{U}(k) \right] \Bigg] \quad (49) \end{aligned}$$

$$\text{subject to} \quad \boldsymbol{\Omega} \Delta \boldsymbol{U}(k) \le \boldsymbol{\omega} \quad (50)$$

### 4.1. Linear Interpolation of the Scheduled Parameters

The scheduled parameters $\lambda^{low}_{em1}, \lambda^{high}_{em1}, \lambda^{low}_{em2}, \lambda^{high}_{em2}$ are calculated by the actually measured $\omega_{em1}(t)$, $\omega_{em2}(t)$. The scheduled parameters are defined near of the maximum rotational speed and the minimum rotational speed as

$$\omega^{low}_{em1} - \delta \le \omega_{em1}(t) \le \omega^{low}_{em1} + \delta, \lambda^{low}_{em1} = 1, \lambda^{high}_{em1} = 0 \quad (51)$$
$$\omega^{high}_{em1} - \delta \le \omega_{em1}(t) \le \omega^{high}_{em1} + \delta, \lambda^{low}_{em1} = 0, \lambda^{high}_{em1} = 1 \quad (52)$$
$$\omega^{low}_{em2} - \delta \le \omega_{em2}(t) \le \omega^{low}_{em2} + \delta, \lambda^{low}_{em2} = 1, \lambda^{high}_{em2} = 0 \quad (53)$$
$$\omega^{high}_{em2} - \delta \le \omega_{em2}(t) \le \omega^{high}_{em2} + \delta, \lambda^{low}_{em2} = 0, \lambda^{high}_{em2} = 1 \quad (54)$$

where $\delta$ is an acceptable error. The scheduled parameters in between the maximum rotational speed and the minimum rotational speed are considered by using a linear interpolation as shown in Fig. 5.

$$\lambda^{high}_{em1}(t) = \frac{\omega_{em1}(t) - \omega^{low}_{em1} - \delta}{\omega^{high}_{em1} - \omega^{low}_{em1} - 2\delta}, \quad (55)$$
$$\lambda^{low}_{em1}(t) = 1 - \lambda^{high}_{em1}(t), \quad (56)$$
$$\lambda^{high}_{em2}(t) = \frac{\omega_{em2}(t) - \omega^{low}_{em2} - \delta}{\omega^{high}_{em2} - \omega^{low}_{em2} - 2\delta}, \quad (57)$$
$$\lambda^{low}_{em2}(t) = 1 - \lambda^{high}_{em2}(t). \quad (58)$$

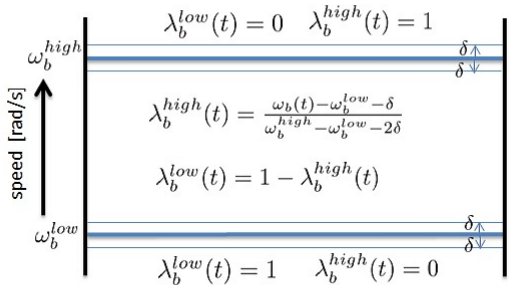


Fig. 5 Linear interpolation

# 5. SIMULATION

### 5.1. Simulation Condition

The proposed approach is validated by numerical simulations. A software application called GT-suite in Matlab Simulink is used to simulate. The target vehicle speed as shown in Fig. 6. The driving environment does not consider traffic congestion, weather, or the grade of the roadway. Case 1 is the result by the proposed method, and Case 2 is the result by Rule Base.

$$\boldsymbol{R} = diag(1.0 \times 10^{-8}, 1.0 \times 10^{-8}, 1.0 \times 10^{-8}) \quad (59)$$
$$\boldsymbol{Q} = diag(1, 1, 1, 1) \quad (60)$$

### 5.2. Simulation Result

The simulation results of Case 1 and Case 2 are indicated in Figs. 8∼15. The actual vehicle speed is intended to follow the target vehicle speed in both cases. The *soc* is controlled within the constraints. By the proposed method, the engine is operated at the optimal point.

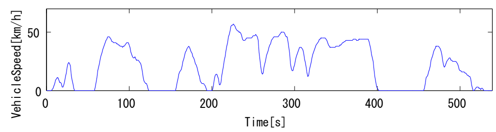


Fig. 6 Target vehicle speed

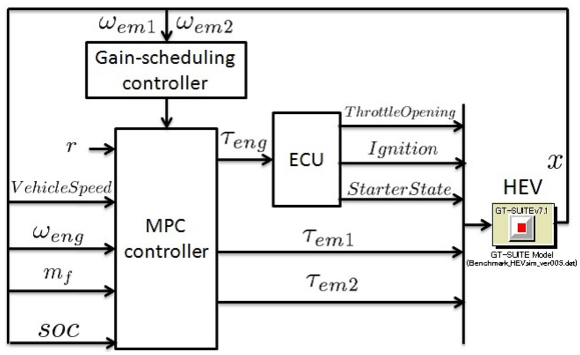


Fig. 7 Simulation block

Table 1 Simulation parameters

| Symbol | Parameter | Value |
|---|---|---|
| $I_{em1}$ | inertia moment of EM1[kg · m$^2$] | 0.0265 |
| $I_{em2}$ | inertia moment of EM2 [kg · m$^2$] | 0.035 |
| $I_{eng}$ | inertia moment of enjine [kg · m$^2$] | 0.16 |
| $R_s$ | sun gear radius[m] | 0.30 |
| $R_r$ | ring gear radius[m] | 0.78 |
| $R_w$ | tire radius[m] | 0.2982 |
| $G_f$ | differential gear ratio | 4.113 |
| $A_f$ | vehicle frontal area[m$^2$] | 3.8 |
| $M$ | vehicle weight[kg] | 1460 |
| $\mu_r$ | rolling resistance coefficient | 0.015 |
| $C_d$ | air resistance coefficient | 0.33 |
| $g$ | Gravitational acceleration[m/s$^2$] | 9.8 |
| $R_{batt}$ | battery resistance[Ω] | 36 |
| $C_{batt}$ | battery capacity[Ah] | 6.5 |
| $V_{oc}$ | open circuit voltage[V] | 221.62 |
| $soc^0$ | the initial value of the soc[%] | 60 |
| $E_0$ | fuel consumption coefficient | 0.077 |
| $T_s$ | sampling time[s] | 0.02 |
| $H_p$ | predictive horizon[step] | 5 |
| $H_u$ | control horizon[step] | 3 |
| $S_o$ | battery coefficient | -0.0007 |

The fuel economy and *soc* of Case 1 and Case 2 are indicated in Table 2. Case 1 improved 5.11% over Case 2. The *soc* is almost the same in both cases.

## 6. CONCLUSIONS

In this paper, we have proposed the fuel consumption optimization for a power-split HEV via gain-scheduled model predictive control. The proposed controller can improve fuel economy over the Rule Base and express the time-varying battery state. Also, the vehicle speed and the *soc* is considered by the controller. But in the case, we don't consider about the engine characteristic. These factors and the start time of the engine should be considered in the future.

## REFERENCES

[1] A. Sciarretta, L. Guzzella, "Control of hybrid electric vehicle", *IEEE Control Systems Magazine*, vol. 27, no. 2, pp. 60-70, 2007.

[2] H. Borhan, A. Vahidi, Anthony M. Phillips, Ming L. Kuang, Ilya V. Kolmanovsky, Stefano Di. Cairano, "MPC-Based Energy Management of a Power-Split Hybrid Electric Vehicle", *IEEE Transactions on Control Systems Technology*, vol. 20, no. 3, pp. 593-603, 2012.

[3] P. Pisu and G. Rizzoni, "A Comparative Study Of Supervisory Control Strategies for Hybrid Electric Vehicles", *IEEE Transactions on Control Systems Technology*, vol. 15, no. 3, pp. 506-518, 2007.

[4] S. G. Li, S. M. Sharkh, F. C. Walsh, C. N. Zhang, "Energy and Battery Management of a Plug-In Series Hybrid Electric Vehicle Using Fuzzy Logic", *IEEE Transactions on Vehicular Technology*, vol. 60, no. 8, pp. 3571-3585, 2011.

[5] N. Kim, S. Cha, H. Peng, "Optimal Control of Hybrid Electric Vehicles Based on Pontryagin's Minimum Principle", *IEEE Transactions on Control Systems Technology*, vol. 19, no. 5, pp. 1279-1287, 2011.

[6] Yuji Yasui, "JSAE-SICE Benchmark Problem II-Fuel Consumption Optimization of Commuter Vehicle Using Hybrid Powertrain", The Technical Committee on Vehicle Control and Modeling, 2012.

[7] Liuping Wang, "Gain-scheduling Model Predictive Control", *Proc. of American Control Conference*, Melbourne, Australia, 2013.

[8] H. Borhan, A. Vahidi, Anthony M. Phillips, Ming L. Kuang, Ilya V. Kolmanovsky, "Predictive Energy Management of a Power-Split Hybrid Electric Vehicle", *2009 American Control Conference*, St. Louis, MO, USA, pp. 3970-3976, 2009.

[9] B. Mashadi, Seyed A. M. Emadi, "Dual-Mode Power-Split Transmission for Hybrid Electric Vehicles", *IEEE Transactions on Vehicular Technology*, vol. 59, no. 7, pp. 3223-3232, 2010.

[10] Jan M. Maciejowski, "*Predictive Control with Constraints*", Pearson Education Limited, 2002.

Table 2 Fuel economy and soc

| | Case 1 Proposed | Case 2 Rule Base |
|---|---|---|
| Fuel economy | 23.67[km/L] | 22.52[km/L] |
| *soc* | 59.39[%] | 59.21[%] |

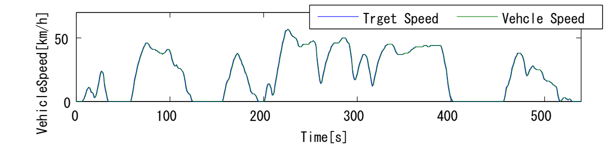

Fig. 8 Case 1 vehicle speed

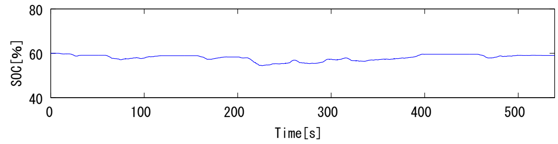

Fig. 9 Case 1 soc

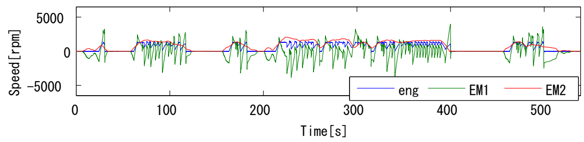

Fig. 10 Case 1 rotational speed

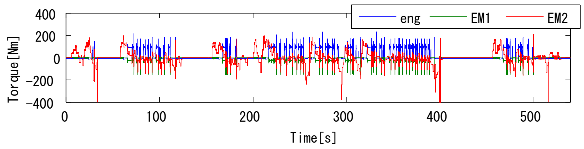

Fig. 11 Case 1 torque

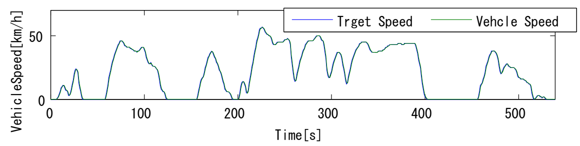

Fig. 12 Case 2 vehicle speed

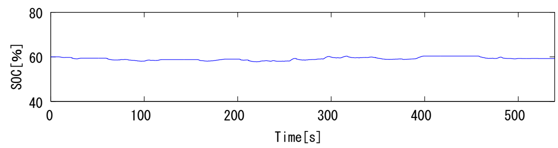

Fig. 13 Case 2 soc

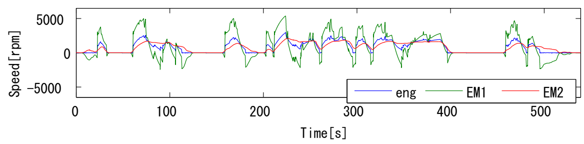

Fig. 14 Case 2 rotational speed

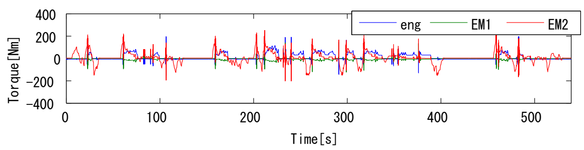

Fig. 15 Case 2 torque